J Fluoresc (2011) 21:231–237
DOI 10.1007/s10895-010-0710-5

ORIGINAL PAPER

Dynamics of $tRNA^{tyr}$ Probed with Long-Lifetime Metal-Ligand Complexes

Woo Suk Hwang · Yun Hong Jung · Woo Sung Son · Byeng Wha Son · Jung Sook Kang

Received: 11 March 2010 / Accepted: 12 August 2010 / Published online: 21 August 2010

Abstract The metal-ligand complexes, $[Ru(bpy)_2(dppz)]^{2+}$ (bpy = 2,2′-bipyridine, dppz = dipyrido[3,2-a:2′,3′-c]phenazine) (RuBD) and $[Ru(phen)_2(dppz)]^{2+}$ (phen = 1,10-phenanthroline) (RuPD), display favorable photophysical properties including long lifetime, polarized emission, and very little background fluorescence. To check if RuBD and RuPD reflect the overall rotational mobility of small nucleic acid, we measured the intensity and anisotropy decays of RuBD and RuPD when intercalated into $tRNA^{tyr}$ using pBC SK(+) phagemid as a control. We used frequency-domain fluorometry with a blue light-emitting diode (LED) as the modulated light source. We observed shorter lifetimes for $tRNA^{tyr}$ than those for the pBC SK(+) phagemid for both probes, however, RuPD showed much larger decrease in the mean lifetime values (64%). The slow rotational correlation time of RuBD (31.3 ns) and the fast rotational correlation time of RuPD (26.0 ns) reflected the overall rotational mobility of $tRNA^{tyr}$. In addition, the steady-state anisotropy and time-resolved anisotropy decay data showed a clear difference between $tRNA^{tyr}$ and pBC SK(+) phagemid. This suggests the possibility of a homogeneous assay for identifying target nucleic acids and/or nucleic acid binding proteins.

Keywords Long-lifetime metal-ligand complex · $tRNA^{tyr}$ · Anisotropy decay · Light-emitting diode · Homogeneous assay

W. S. Hwang · Y. H. Jung · J. S. Kang (✉)
Department of Oral Biochemistry and Molecular Biology,
School of Dentistry, Pusan National University,
Yangsan 626-870, South Korea
e-mail: jsokang@pusan.ac.kr

W. S. Son
Department of Orthodontics, School of Dentistry,
Pusan National University,
Yangsan 626-870, South Korea
e-mail: wsson@pusan.ac.kr

B. W. Son
Department of Chemistry, Pukyong National University,
Busan 608-737, South Korea
e-mail: sonbw@pknu.ac.kr

Introduction

Long-lifetime metal-ligand complexes (MLCs), which display decay times ranging from 100 ns to more than 10 μs, show several characteristics that make them versatile biophysical probes [1–4]. Because of the large Stokes' shift, the MLCs do not display significant radiative or nonradiative homotransfer [2, 3]. In general, the MLCs display reasonably good water solubility and high thermal, chemical, and photochemical stability [2, 3]. Most MLCs display polarized emission, making them useful for microsecond hydrodynamics. Finally, if needed, the long lifetimes of the MLCs allow the use of gated detection, which can be employed to suppress interfering autofluorescence from biological samples and can thus provide improved sensitivity [5].

Barton and co-workers [6–8] reported the use of the dipyrido[3,2-a:2′,3′-c]phenazine (dppz) complexes of ruthenium as a spectroscopic probe for nucleic acids because of their "molecular light switch" properties for DNA. Since the luminescent enhancement upon DNA binding is $\geq 10^4$, there is essentially no background with the dppz complexes of ruthenium. There are two common dppz complexes of ruthenium, the 2,2′-bipyridine (bpy) derivative $[Ru(bpy)_2(dppz)]^{2+}$ (RuBD) and the 1,10-phenanthroline (phen) derivative $[Ru(phen)_2(dppz)]^{2+}$ (RuPD). Because both complexes display large fundamental anisotropies

(r_0), Lakowicz and co-workers introduced the use of these MLCs to measure the dynamics of DNA. Jenkins *et al*. [7] reported RuBD's superiority over RuPD in the sensitivity to conformational differences in DNA because of the incomplete shielding of the dppz ligand from water in the presence of bpy in contrast to the other phen derivative RuPD. Thus, most anisotropy decay measurements were performed using RuBD [9–12]. RuBD was utilized to measure the anisotropy decays of calf thymus DNA [9, 10] and supercoiled, linear, and relaxed pTZ18U plasmids [11, 12]. Using RuPD, the anisotropy decays of calf thymus DNA [10] and pBluescript II SK(+) phagemid [13] were determined.

In the present study, we measured the intensity and anisotropy decays of RuBD and RuPD intercalated into $tRNA^{tyr}$. For a comparison, the intensity and anisotropy decays of RuBD and RuPD intercalated into pBC SK(+) phagemid were investigated as well. The aim of this research is three-fold: (1) to check if both RuBD and RuPD reflect the overall rotational mobility of small nucleic acid such as $tRNA^{tyr}$; (2) to check the photophysical differences between RuBD and RuPD when intercalated into $tRNA^{tyr}$ and pBC SK(+) phagemid; and (3) to check whether RuBD and RuPD clearly show the size difference between $tRNA^{tyr}$ and pBC SK(+) phagemid. All measurements were done using an inexpensive blue light-emitting diode (LED) as the modulated light source. LEDs are easily modulated up to hundreds of MHz [14]. The combination of the use of long-lifetime MLCs with a blue LED allowed us to perform time-resolved intensity and anisotropy decay measurements with a simpler and lower-cost instrument.

Materials and Methods

Materials LB-medium from Beckton, Dickinson and Company (Franklin Lakes, NJ, USA); $tRNA^{tyr}$, agarose and chloramphenicol from Sigma (St. Louis, MO, USA); pBC SK(+) phagemid (3.4 kb) and *E. coli* XL1-Blue MRF′ from Stratagene (La Jolla, CA, USA); and plasmid mega kit from Qiagen Inc. (Valencia, CA, USA). $tRNA^{tyr}$ was used without further purification. RuBD and RuPD were synthesized by the method described previously [9, 10]. All other chemicals were of the reagent grade, and water was deionized with a Milli-Q system. For $tRNA^{tyr}$, all measurements were done in 100 mM KCl, 10 mM Tris, pH 7.4. In the case of pBC SK(+) phagemid, fluorescence measurements were carried out in 5 mM Tris, pH 7.4, containing 50 mM NaCl.

Absorption and steady-state fluorescence measurements pBC SK(+) phagemids were purified with Qiagen plasmid mega kit from 500 ml overnight cultures of *E. coli* XL1-Blue MRF′ in LB-medium containing chloramphenicol. About 5–10 mM stock solution of RuBD and RuPD were prepared in dimethylformamide (DMF). The effect of DMF was negligible because we used very low concentrations of DMF (0.1–0.4% v/v). The $tRNA^{tyr}$ concentration was 1 mM nucleotide while that of phagemid was 300 μM bp. The concentrations of $tRNA^{tyr}$ and DNA were determined using molar extinction coefficients of 7,800 $M^{-1}cm^{-1}$ (expressed as nucleotide) and 13,000 $M^{-1}cm^{-1}$ (expressed as bp) at 260 nm, respectively. The concentrations of RuBD and RuPD were 20 and 15 μM, respectively, and were determined using molar extinction coefficients of 13,000 $M^{-1}cm^{-1}$ at 440 nm and 21,000 $M^{-1}cm^{-1}$ at 440 nm, respectively. UV-visible absorption spectra were measured with an Agilent 8453 diode array spectrophotometer. Steady-state intensity and anisotropy measurements were carried out using a Cary Eclipse fluorescence spectrophotometer (Varian Inc., Palo Alto, CA, USA).

The intensity of the components of the fluorescence that were parallel (I_{VV}) and perpendicular (I_{VH}) to the direction of the vertically polarized excitation light was determined by measuring the emitted light through polarizers oriented vertically and horizontally. The steady-state anisotropy is given by:

$$r = \frac{I_{VV} - GI_{VH}}{I_{VV} + 2GI_{VH}} \tag{1}$$

where G is a grating correction factor for the monochromator's transmission efficiency for vertically and horizontally polarized light. This value is given by the ratio of the fluorescence intensities of the vertical (I_{HV}) to horizontal (I_{HH}) components when the exciting light is polarized in the horizontal direction.

FD intensity and anisotropy decay measurements Measurements were performed with a Koala frequency-domain (FD) lifetime spectrometer (ISS Inc., Champaign, IL, USA) using a blue LED as the excitation source. A 480±20 nm interference filter and a 630 nm cut-off filter were used for isolating excitation and emission, respectively. Rhodamine B in water (τ = 1.68 ns) was utilized as a lifetime standard. All measurements were performed at 25°C.

The intensity decays were recovered from the FD data in terms of a multiexponential model using nonlinear least squares analysis [15, 16]:

$$I(t) = \sum_{i=1}^{n} \alpha_i e^{-t/\tau_i} \tag{2}$$

where the preexponential factor α_i is the amplitude of each component, $\Sigma\alpha_i$ = 1.0, τ_i is the decay time, and n is the

number of exponential components. Mean lifetimes were calculated by:

$$< \tau >= \frac{\sum_i \alpha_i \tau_i^2}{\sum_i \alpha_i \tau_i} = \sum_i f_i \tau_i \quad (3)$$

where f_i is the fractional steady-state contribution of each component to the total emission, and Σf_i is normalized to unity. f_i is given by:

$$f_i = \frac{\alpha_i \tau_i}{\sum_j \alpha_j \tau_j} \quad (4)$$

The best fits were obtained by minimizing χ_R^2 values:

$$\chi_R^2 = \frac{1}{\nu} \sum_\omega \left[\left(\frac{\phi_\omega - \phi_{c\omega}}{\delta \phi} \right)^2 + \left(\frac{m_\omega - m_{c\omega}}{\delta m} \right)^2 \right] \quad (5)$$

where ν is the number of degrees of freedom, and ϕ_ω and m_ω are the experimental phase and modulation, respectively. The subscript c is used to indicate calculated values for assumed values of α_i and τ_i, and $\delta\phi$ and δm are the experimental uncertainties.

The FD anisotropy decays were also analyzed in terms of the multiexponential model using nonlinear least squares analysis [17, 18]:

$$r(t) = \sum_i r_0 g_i e^{-t/\theta_i} \quad (6)$$

where g_i is the amplitude of the anisotropy component with a rotational correlation time θ_i, $\Sigma g_i = 1.0$, and r_0 is the anisotropy in the absence of rotational diffusion. The total anisotropy r_0 was a fitted parameter. The modulated anisotropy r_ω was calculated by:

$$r_\omega = \frac{\Lambda_\omega - 1}{\Lambda_\omega + 2} \quad (7)$$

where Λ_ω is the ratio of the amplitude of the parallel and the perpendicular components of the modulated emission.

Results and Discussion

Steady-State Intensity and Anisotropy

Figure 1 shows the chemical structures of RuBD and RuPD. The normalized fluorescence spectra of RuBD and RuPD intercalated into the $tRNA^{tyr}$ and pBC SK(+) phagemid are shown in Fig. 2. Both complexes showed emission peaks at about 620 nm, and there was little difference between the $tRNA^{tyr}$ and pBC SK(+) phagemid. In aqueous solution the luminescence of these probes is undetectable. As expected, we observed lower steady-state anisotropy values with RuPD than RuBD because of its longer lifetime (Fig. 3). For both probes $tRNA^{tyr}$ showed much lower steady-state anisotropy values because of its small size (Fig. 3). Since the steady-state anisotropy values were quite low, it is not likely that both RuBD and RuPD are suitable for measuring the steady-state anisotropy values of small nucleic acids such as $tRNA^{tyr}$. However, both RuBD and RuPD clearly showed the size difference between $tRNA^{tyr}$ and pBC SK(+) phagemid.

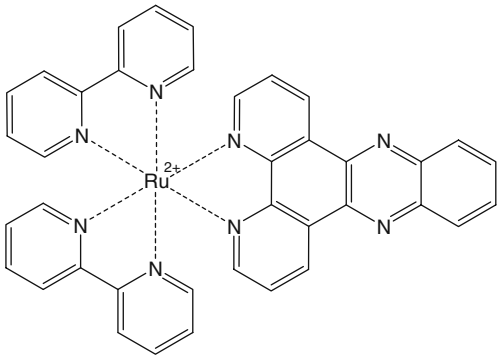

$[Ru(bpy)_2(dppz)]^{2+}$ (RuBD)

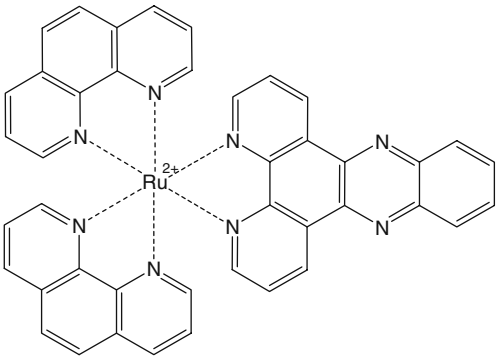

$[Ru(phen)_2(dppz)]^{2+}$ (RuPD)

Fig. 1 Chemical structures of $[Ru(bpy)_2(dppz)]^{2+}$ (RuBD) and $[Ru(phen)_2(dppz)]^{2+}$ (RuPD)

Intensity Decays

The FD intensity decays of RuBD and RuPD intercalated into $tRNA^{tyr}$ and pBC SK(+) phagemid are shown in Fig. 4. For both probes the intensity decays were best fit by a triple exponential decay. Table 1 shows the intensity decay results for RuBD and RuPD intercalated into $tRNA^{tyr}$ and pBC SK (+) phagemid. In the case of RuBD, the mean lifetime values for the $tRNA^{tyr}$ and pBC SK(+) phagemid were 102.2 and 129.2 ns, respectively. However, using RuPD, we observed much shorter lifetime for $tRNA^{tyr}$ (170.3 ns)

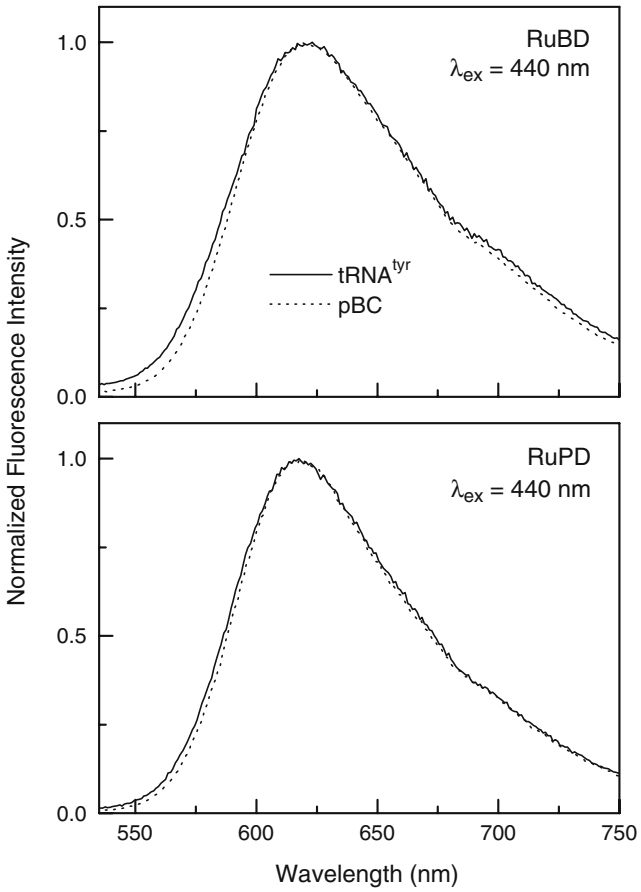

Fig. 2 Emission spectra of RuBD (top) and RuPD (bottom) intercalated into $tRNA^{tyr}$ and pBC SK(+) phagemid

than that for the pBC SK(+) phagemid (474.9 ns). For RuBD and RuPD, the lifetime values decreased about 21% and 64%, respectively, in the $tRNA^{tyr}$. Jenkin *et al.* [7] also reported a large decrease in the mean lifetime of RuPD when intercalated into $tRNA^{phe}$. This result indicates that the RuPD MLC was much more exposed to water in the $tRNA^{tyr}$ than in the phagemid, resulting in a far shorter lifetime. Thus, it seems that $tRNA^{tyr}$ adopts a lot less favorable conformations for RuPD intercalation than the phagemid.

Dynamics of $tRNA^{tyr}$

In addition to the intensity decay measurements, we also measured the anisotropy decays of RuBD and RuPD intercalated into $tRNA^{tyr}$ and pBC SK(+) phagemid. As shown in Figs. 5 and 6, there were large differences in the values of both modulated anisotropy and differential phase between $tRNA^{tyr}$ and pBC SK(+) phagemid. For both probes, the best fits of the anisotropy decay data were obtained using the two correlation time model, and the results are summarized in Table 2. In the case of RuBD intercalated into $tRNA^{tyr}$, the slow rotational correlation time (31.3 ns) appears to be consistent with that expected for overall rotational mobility of $tRNA^{tyr}$. The fast rotational correlation time (10.3 ns) may be due to independent motion of two helical arms of the L-shaped structure of $tRNA^{tyr}$ because the correlation time constant of local internal motion of the bases within tRNA is usually in the range of picoseconds [19]. For RuPD, the slow and fast rotational correlation times were 106.6 and 26.0 ns, respectively, when intercalated into $tRNA^{tyr}$ (Table 2). The fast rotational correlation time (26.0 ns) is comparable to the slow rotational correlation time using RuBD (31.3 ns). Thus, it is likely that the fast rotational correlation time of RuPD is consistent with the overall rotational mobility of $tRNA^{tyr}$. The slow rotational correlation time of RuBD (31.3 ns) was longer than the fast rotational correlation time using RuPD (26.0 ns) or the value reported previously for $tRNA^{tyr}$ by electro-optical measurements [20]. This suggests the possibility of the presence of somewhat denatured extended form of $tRNA^{tyr}$ using RuBD. A plausible explanation may be the probe concentration, about 1.7:1 of RuBD to $tRNA^{tyr}$ molar ratio. Because of very low quantum yield (Q = 0.008) of RuBD [21], quite high probe concentration was used. In the case of RuPD, the probe to

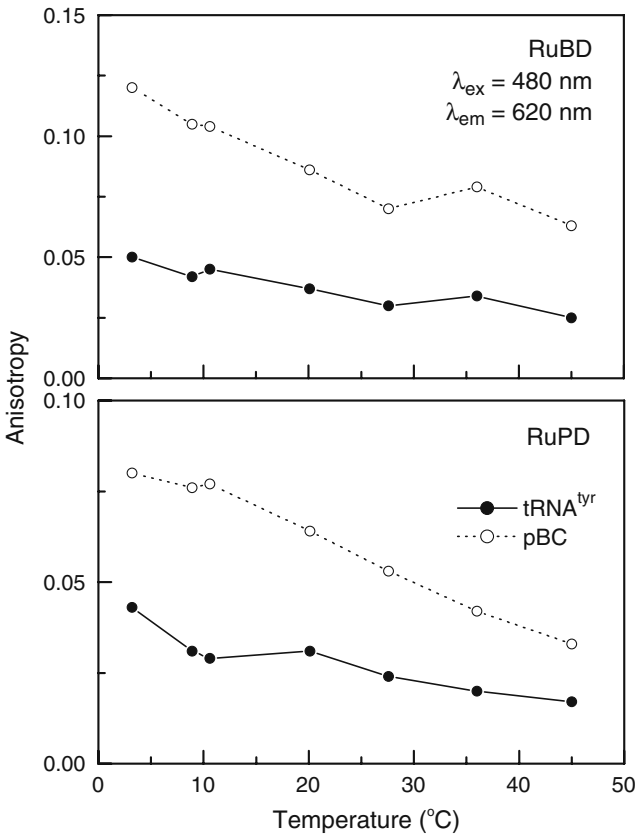

Fig. 3 Temperature-dependent steady-state anisotropy of RuBD (top) and RuPD (bottom) intercalated into $tRNA^{tyr}$ and pBC SK(+) phagemid. The steady-state anisotropy values were calculated by Eq. 1

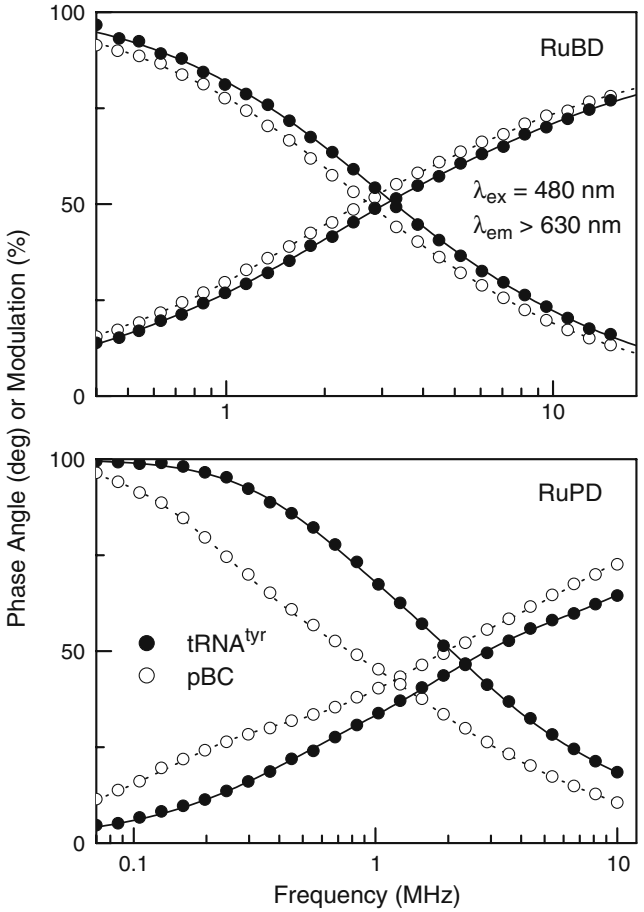

Fig. 4 Intensity decays of RuBD (top) and RuPD (bottom) intercalated into $tRNA^{tyr}$ and pBC SK(+) phagemid. The symbols represent the measured phase and modulation values. The *solid lines* show the best multiexponential fits to the data

$tRNA^{tyr}$ molar ratio was 1.3:1 because the quantum yield of RuPD (Q = 0.017) [22] is more than twice that of RuBD [21]. However, the slow rotational correlation time of RuPD (106.6 ns) implies the presence of aggregates of the $tRNA^{tyr}$-RuPD complex. Thus, the $tRNA^{tyr}$-RuPD complex does not seem to be as stable as the $tRNA^{tyr}$-RuBD complex because of the bigger size and increased hydrophobicity of the phen group. The absence of Mg^{2+} in the buffer, which plays an important role in tRNA conformation, can be a factor of the possibilities of the presence of somewhat denatured extended form of $tRNA^{tyr}$ using RuBD and aggregates of the $tRNA^{tyr}$-RuPD complex as well. Figures 5 and 6 (first panel) also show the modulated anisotropy values for RuBD and RuPD intercalated into the $tRNA^{tyr}$ and pBC SK(+) phagemid. We observed lower modulated anisotropy values using RuPD than RuBD, which is in agreement with the results of our steady-state anisotropy measurements. For both probes $tRNA^{tyr}$ showed lower modulated anisotropy values, which also coincides with our steady-state anisotropy results (Figs. 5 and 6).

Dynamics of pBC SK(+) Phagemid

For the pBC SK(+) phagemid, the slow and fast rotational correlation times appear to be consistent with the bending and torsional motions of phagemids, respectively, for both probes. The torsional motion of DNA occurs in 1–100 ns, while the bending motion of DNA ranges from about 100 ns to more than 100 μs [23]. Using both RuBD and RuPD, we obtained similar values of the slow and fast rotational correlation times to those reported previously for pTZ18U plasmid (2,860 bp) [11, 12] and pBluscript II SK(+) phagemid (2,961 bp) [13] because the differences in bps were small (Table 2). The important point is that RuBD and RuPD have different time windows of the torsional and bending motions of phagemid/plasmid. For RuBD, the bending and torsional motions occurred in the range of about 300–400 and 15–30 ns, respectively. Using RuPD, the values of about 1 μs and 40 ns of the bending and torsional motions, respectively, were obtained.

The Use of Long-Lifetime MLCs as Probes of Nucleic Acid Dynamics

The fluorescence spectroscopic method is an indirect way of measuring nucleic acid dynamics. As discussed in the above section, the types and/or the time windows of nucleic acid motions reflected by the probes are different depending on the probes. Information on the rotational motion is

Table 1 Multiexponential intensity decay analyses of $[Ru(bpy)_2(dppz)]^{2+}$ (RuBD) and $[Ru(phen)_2(dppz)]^{2+}$ (RuPD) intercalated into $tRNA^{tyr}$ and pBC SK(+) phagemid

MLC	Nucleic acid	τ_i (ns)	α_i	f_i[a]	$<\tau>$[a] (ns)	χ_R^2[b]
RuBD	$tRNA^{tyr}$	225.2	0.07	0.23	102.2	2.0
		73.5	0.55	0.63		
		23.5	0.38	0.14		
	pBC	335.5	0.04	0.19	129.2	1.3
		90.8	0.57	0.67		
		28.2	0.39	0.14		
RuPD	$tRNA^{tyr}$	305.3	0.10	0.44	170.3	2.3
		79.9	0.39	0.45		
		15.0	0.51	0.11		
	pBC	793.8	0.10	0.54	474.9	1.6
		119.5	0.40	0.35		
		29.3	0.50	0.11		

[a] Fractional intensities f_i and mean lifetimes $<\tau>$ were calculated using Eqs. 4 and 3, respectively

[b] The χ_R^2 values were calculated by Eq. 5, and the standard errors of phase angle and modulation were set at 0.2° and 0.005, respectively

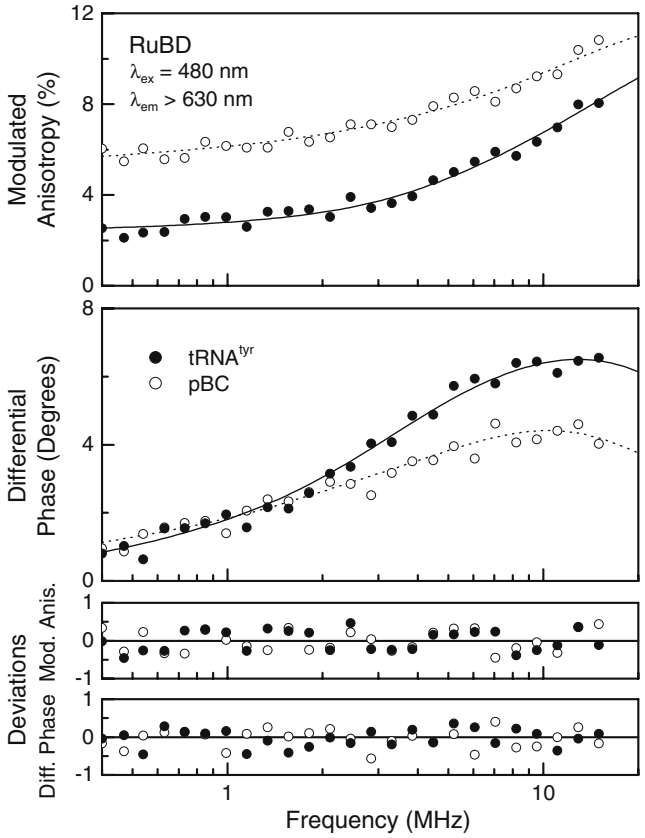

Fig. 5 Anisotropy decays of RuBD intercalated into $tRNA^{tyr}$ and pBC SK(+) phagemid. The symbols in the first and second panels represent the modulated anisotropy and the measured phase shift values, respectively. The modulated anisotropy values were calculated from measured Λ_ω using Eq. 7. The solid lines show the best multiexponential fits to the data. The lower two panels show plots of the residuals between the experimental data and the fitted curve

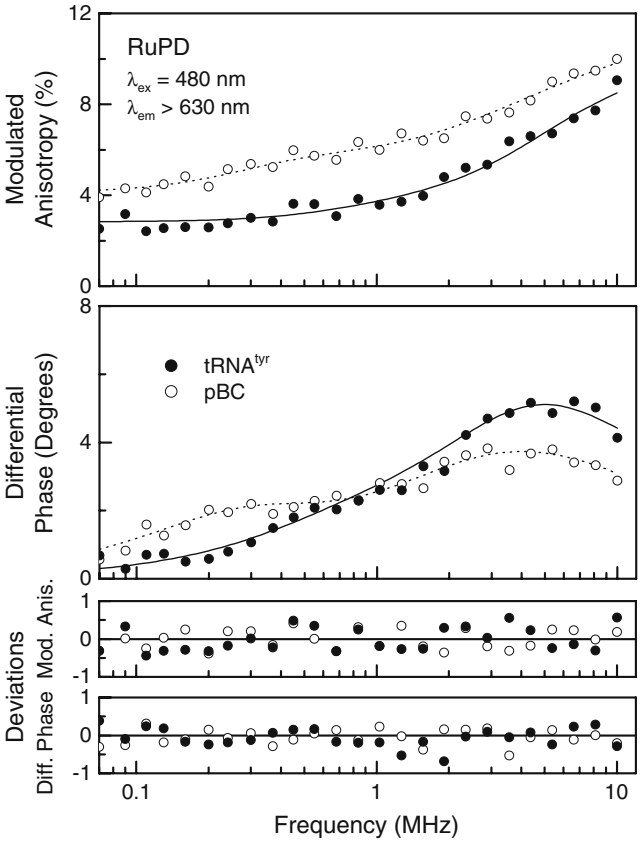

Fig. 6 Anisotropy decays of RuPD intercalated into $tRNA^{tyr}$ and pBC SK(+) phagemid. All conditions are the same as in Fig. 5

usually available over a time scale not exceeding three times the lifetime of the fluorophores. Hence, it is not possible to measure the bending motions of DNA accurately using conventional nucleic acid probes that have lifetime values of about 5–20 ns. Clearly no single fluorescent probe can encompass the diversity and complexity inherent in the problems of nucleic acid dynamics. A variety of fluorescent probes that differ in lifetimes, binding specificity, etc., must be applied together and their results combined.

The long-lifetime MLCs are valuable because, among novel fluorophores, they are the only group of fluorophores that have significant potential as a useful tool for investigating the hydrodynamics of biological macromolecules. Lanthanides show much longer lifetimes than MLCs, however, they do not show polarized emission. The quantum dots show a number of characteristics that make them the prime candidates in many fluorescence studies recently, but they do not seem to be well suited for polarization measurements because of their big size and their shape. It may be premature to take sides in the controversy about whether RuBD or RuPD is more promising. It seems that both RuBD and RuPD have their own merits and demerits as described in the above sections. It is expected that both RuBD and RuPD may find their appropriate uses in a wide variety of applications.

Table 2 Multiexponential anisotropy decay analyses of $[Ru(bpy)_2(dppz)]^{2+}$ (RuBD) and $[Ru(phen)_2(dppz)]^{2+}$ (RuPD) intercalated into $tRNA^{tyr}$ and pBC SK(+) phagemid

MLC	Nucleic acid	θ_i (ns)	r_0*g(i)	Σ (r_0*g(i))	$\chi_R^{2\,a}$
RuBD	$tRNA^{tyr}$	31.3	0.054	0.121	2.4
		10.3	0.067		
	pBC	344.5	0.057	0.124	2.9
		17.1	0.067		
RuPD	$tRNA^{tyr}$	106.6	0.020	0.107	3.3
		26.0	0.087		
	pBC	951.7	0.041	0.110	2.2
		38.2	0.069		

[a] The χ_R^2 values were calculated by Eq. 5, and the standard errors of phase angle and modulation were set at 0.2° and 0.005, respectively

The Possibility of a Homogeneous Assay for Identifying Target Nucleic Acids and/or Nucleic Acid Binding Proteins

In the present study, the steady-state anisotropy and time-resolved anisotropy decay data showed a distinct difference between $tRNA^{tyr}$ and pBC SK(+) phagemid (Figs. 3, 5 and 6, Table 2). Both RuBD and RuPD showed almost zero anisotropy values when intercalated into $tRNA^{tyr}$ because of the long-lifetimes, however, when intercalated into pBC SK(+) phagemid, the anisotropies of RuBD and RuPD increased 2.3- and 2.1-fold, respectively, at 20°C (Fig. 3). This suggests the possibility of a homogeneous assay. The oligonucleotide probes are labelled with either RuBD or RuPD, and they will show almost negligible steady-state anisotropy values. When target DNA/RNA or DNA/RNA binding proteins are bound to the probes, the steady-state anisotropy values will increase. The larger molecules will show more significant increase in steady-state anisotropies. The time-resolved anisotropy decay measurements will confirm the steady-state anisotropy data. In this way, the presence of target DNA/RNA and/or DNA/RNA binding proteins can be easily determined with high sensitivity. The non-separation, one-step homogeneous assay will reduce the risk of contamination and eliminate labor-intensive and time-consuming washing steps/sample handling, which are commonly encountered in conventional heterogeneous assays. This assay may be useful in clinical diagnosis and biological and biomedical studies. Further experimentation is required to verify the above hypothesis.

Conclusion

Our data clearly showed that both RuBD and RuPD can be useful for studying hydrodynamics of small nucleic acid such as $tRNA^{tyr}$.

Acknowledgments This research was supported by Medical Research Institute Grant (2003-33), Pusan National University.

References

1. DeGraff BA, Demas JN (1994) Direct measurement of rotational correlation times of luminescent ruthenium(II) molecular probes by differential polarized phase fluorometry. J Phys Chem 98:12478–12480
2. Terpetschnig E, Szmacinski H, Lakowicz JR (1997) Long-lifetime metal-ligand complexes as probes in biophysics and clinical chemistry. Methods Enzymol 278:295–321
3. Lakowicz JR, Gryczynski I, Piszczek G, Tolosa L, Nair R, Johnson ML, Nowaczyk K (2000) Microsecond dynamics of biological molecules. Methods Enzymol 323:473–509
4. Piszczek G (2006) Luminescent metal-ligand complexes as probes of macromolecular interactions and biopolymer dynamics. Arch Biochem Biophys 453:54–62
5. Haugen GR, Lytle FE (1981) Quantitation of fluorophores in solution by pulsed laser excitation of time-filtered detection. Anal Chem 53:1554–1559
6. Friedman AE, Chambron J-C, Sauvage J-P, Turro NJ, Barton JK (1990) Molecular "light switch" for DNA: $Ru(bpy)_2(dppz)^{2+}$. J Am Chem Soc 112:4960–4962
7. Jenkin Y, Friedman AE, Turro NJ, Barton JK (1992) Characterization of dipyridophenazine complexes of ruthenium(II): the light switch effect as a function of nucleic acid sequence and conformation. Biochemistry 31:10809–10816
8. Murphy CJ, Barton JK (1993) Ruthenium complexes as luminescent reporters of DNA. Methods Enzymol 226:576–594
9. Lakowicz JR, Malak H, Gryczynski I, Castellano FN, Meyer GJ (1995) DNA dynamics observed with long lifetime metal-ligand complexes. Biospectroscopy 1:163–168
10. Malak H, Gryczynski I, Lakowicz JR, Meyers GJ, Castellano FN (1997) Long-lifetime metal-ligand complexes as luminescent probes for DNA. J Fluoresc 7:107–112
11. Kang JS, Abugo OO, Lakowicz JR (2002) Dynamics of supercoiled and linear pTZ18U plasmids observed with a long-lifetime metal-ligand complex. Biopolymers 67:121–128
12. Kang JS, Abugo OO, Lakowicz JR (2002) Dynamics of supercoiled and relaxed pTZ18U plasmids probed with a long-lifetime metal-ligand complex. J Biochem Mol Biol 35:389–394
13. Kang JS, Son BW, Choi HD, Yoon JH, Son WS (2005) Dynamics of supercoiled and linear pBluscript II SK(+) phagemids probed with a long-lifetime metal-ligand complex. J Biochem Mol Biol 38:104–110
14. Sipior J, Carter JM, Lakowicz JR, Rao G (1996) Single quantum well light-emitting diodes demonstrated as excitation sources for nanosecond phase modulation fluorescence lifetime measurements. Rev Sci Instrum 67:3795–3798
15. Gratton E, Limkeman M, Lakowicz JR, Maliwal BP, Cherek H, Laczko G (1984) Resolution of mixtures of fluorophores using variable-frequency phase and modulation data. Biophys J 46:479–486
16. Lakowicz JR, Laczko G, Cherek H, Gratton E, Limkeman M (1984) Analysis of fluorescence decay kinetics from variable-frequency phase-shift and modulation data. Biophys J 46:463–477
17. Lakowicz JR, Gryczynski I (1991) Frequency-domain fluorescence spectroscopy. In: Lakowicz JR (ed) Topics in fluorescence spectroscopy, vol. 1: techniques. Plenum, New York, pp 293–355
18. Lakowicz JR, Cherek H, Kusba J, Gryczynski I, Johnson ML (1993) Review of fluorescence anisotropy decay analysis by frequency-domain fluorescence spectroscopy. J Fluoresc 3:103–116
19. Patkowski A, Eimer W, Dorfmüller T (1990) Internal dynamics of $tRNA^{phe}$ studied by depolarized dynamic light scattering. Biopolymers 30:975–983
20. Porschke D, Antosiewicz J (1990) Permanent dipole moment of tRNA's and variation of their structure in solution. Biophys J 58:403–411
21. Lakowicz JR, Piszczek G, Kang JS (2001) On the possibility of long-wavelength long-lifetime high-quantum yield luminophores. Anal Biochem 288:62–75
22. Kang JS, Lakowicz JR (2001) Fluorescence resonance energy transfer in calf thymus DNA from a long-lifetime metal-ligand complex to nile blue. J Biochem Mol Biol 34:551–558
23. Schurr JM, Fujimoto BS, Wu P, Song L (1992) Fluorescence studies of nucleic acids: dynamics, rigidities, and structures. In: Lakowicz JR (ed) Topics in fluorescence spectroscopy, vol. 3: biochemical applications. Plenum, New York, pp 137–229